

Tau dephosphorylation and microfilaments disruption are upstream events of the anti-proliferative effects of DADS in SH-SY5Y cells

Katia Aquilano^a, Paola Vigilanza^a, Giuseppe Filomeni^a, Giuseppe Rotilio^{a, b}, Maria R. Ciriolo^{a, b, *}

^a Department of Biology, University of Rome "Tor Vergata", Via della Ricerca Scientifica, 00133, Rome, Italy

^b Research Centre IRCCS San Raffaele, Via dei Bonaccorsi, 00165, Rome, Italy

Received: August 12, 2008; Accepted: October 21, 2008

- Introduction
- Material and methods
 - Material
 - Cell cultures and treatments
 - Microscopy analysis
 - SOD1 enzyme assay
 - Cell fractionation and Western blotting
 - Determination of protein carbonylation
 - Analysis of cell cycle and apoptosis
- Statistical analysis
- Results
 - DADS induces cytoskeletal alterations in SH-SY5Y cells
 - Superoxide is implicated in microfilaments and microtubules disruption
 - DADS induces PP1-mediated Tau dephosphorylation
 - DADS-mediated ROS increase is responsible for Tau dephosphorylation
- Discussion

Abstract

Garlic organosulphur compounds have been successfully used as redox anti-proliferative agents. In this work, we dissect the effects of diallyl disulphide (DADS) focusing on the events upstream of cell cycle arrest and apoptosis induced in neuroblastoma SH-SY5Y cells. We demonstrate that DADS is able to cause early morphological changes, cytoskeleton oxidation, microfilaments reduction and depolymerization of microtubules. These events are attenuated in cells stably overexpressing the antioxidant enzyme SOD1, suggesting that superoxide plays a crucial role in destabilizing cytoskeleton. Moreover, we evidence that the main microtubules-associated protein Tau undergoes PP1-mediated dephosphorylation as demonstrated by treatment with okadaic acid as well as by immunoreaction with anti-Tau-1 antibody, which specifically recognizes its dephosphorylated forms. Tau dephosphorylation is inhibited by the two-electron reductants NAC and GSH ester but not by SOD1. The inability of DADS to induce apoptosis in neuroblastoma-differentiated cells gives emphasis to the anti-proliferative activity of DADS, which can be regarded as a promising potent anti-neuroblastoma drug by virtue of its widespread cytoskeleton disrupting action on proliferating cells.

Keywords: diallyl disulphide • garlic • Tau • microfilaments • microtubules

Introduction

Evidence that garlic derivatives could be employed in the treatment of cancer and other human diseases has been now widely provided. In fact, they are effective in promoting cell cycle arrest and apoptosis in several cancer cells [1], in increasing vasodilatation and inhibiting platelet aggregation and cholesterol synthesis [2]. When garlic is minced or crushed, enzymatic activity of alliinase converts its major constituent alliin into allyl sulphur compounds [3], which are thought to be responsible for its flavour and

aroma, as well as for its potential health benefits. It has been demonstrated that organosulphur derivatives account for the majority of the garlic anti-proliferative effects [4]. Among garlic organosulphurs with the highest anti-proliferative capacity, the water-soluble S-allyl cysteine (SAC) and S-allylmercaptocysteine (SAMC), and the oil-soluble diallyl disulphide (DADS) and triallyl disulphide (DATS) are included. The anti-proliferative effects of garlic organosulphur compounds seem to be related to their

*Correspondence to: Maria Rosa CIRIOLO,
Department of Biology, University of Rome "Tor Vergata", Via della
Ricerca Scientifica, 00133 Rome, Italy.

Tel.: +39 06 7259 4369
Fax: +39 06 7259 4311
E-mail: ciriolo@bio.uniroma2.it

capacity to cause oxidative damage by increasing the production of reactive oxygen species (ROS). We have previously demonstrated that DADS exerts cytotoxic activity on neuroblastoma cells [5, 6], whereas cells well equipped with antioxidants such as adenocarcinoma gastric cells (notably rich in glutathione peroxidase) or neuroblastoma cells overexpressing copper, zinc superoxide dismutase (SOD1) are resistant to DADS [5, 7]. Moreover, we evidenced that DADS commits cells to apoptosis through a mechanism involving a ROS-dependent activation of JNK/c-Jun signalling pathway.

Cytoskeleton is a dynamic component of the cell as it is involved in maintenance of cell shape, intracellular trafficking, cell division, cell migration and adhesion. Cytoskeleton represents one of the preferential targets of ROS due to the relative high abundance of oxidizable residues of its protein constituents. It has been demonstrated that oxidative stress causes both microfilaments and microtubules disruption owing to oxidative modifications of specific methionine and cysteine residues of actin and tubulin [8–11]. Exposure of cells to pro-oxidants agents such as menadione, diamide or *tert*-butyl hydroperoxide results in disruption of microfilament network associated with the preferential oxidation of the conserved Cys³⁷⁴ of actin [8, 12–14]. More recent evidence indicates that also carbonylation may play a role in loss of cytoskeletal function [9, 15]. Moreover, ROS causes a rise in calcium concentration promoting dissociation of actin microfilaments as consequence of calpain-mediated cleavage of actin-binding proteins [16].

Importantly, cytoskeleton and cytoskeleton-associated proteins has been found to have a fundamental role in the processes leading to either stress stimuli resistance or apoptosis. For example, the dramatic morphological changes typical of apoptotic cells are due to a complete reorganization of the cytoskeleton, ensuring the orchestrated breakdown of the cell into apoptotic bodies and the maintenance of intact plasma membrane [17, 18]. Degradation of cytoskeletal proteins such as actin or intermediate filaments due to calpains or caspases activity also plays a crucial role in apoptosis commitment [19–21]. Detachment of microtubules-associated Bim from cytoskeleton is essential for its pro-apoptotic activity into mitochondria [22]; the loss of interaction of NF-E2-related factor-2 (Nrf-2) with the actin-anchored protein Keap1 leads to its nuclear localization and transcription of several cytoprotective and antioxidant genes that enhance cell survival [23]; the tyrosin kinase c-Abl, which has been found to associate with filamentous actin and to have a role in cell motility, inhibits cell differentiation and promotes apoptosis in response to genotoxic stress [24]. Moreover, abnormal phosphorylation of the microtubules-associated protein Tau has been now established to have a causative role in the processes leading to neuronal apoptosis in a variety of neurodegenerative diseases called tauopathies [25].

The use of cytoskeleton-disrupting agents in chemotherapy has been proposed as a strategy to selectively kill tumour cells [26]. Among the most used drugs, there are those belonging to the taxol-like group and Vinka alkaloids, which successfully perturb microtubules dynamics of proliferating cells [27]. In contrast, compounds targeting microfilaments, such as cytochalasins, dis-

play high cytotoxicity and for this reason are not currently employed in cancer treatment [28]. Several pieces of evidence suggest that apoptosis elicited by garlic derivatives is preceded by accumulation of cells in G2/M phase [4–6, 29]. Cell cycle arrest has been linked to direct interaction of garlic derivatives with cytoskeletal components, primarily microtubules. In this context, SAMC, DADS and DATS have been demonstrated to directly oxidize tubulin sulphhydryl groups on specific Cys residues inhibiting mitotic spindle [30–34]. Disrupting effects on microfilaments have not been reported yet, however, allicin treatment causes perturbation of cortical actin polymerization in primary human T cells resulting in inhibition of cell migration [35].

Tau is considered the main microtubules-associated protein responsible for microtubules assembly and stabilization in cells of neuronal origin [36]. Deregulation of its function through altered phosphorylation on Ser or Thr residues has been claimed as the principal cause of cytoskeleton disruption in a number of neurodegenerative disease named tauopathies [25]. Recently, the involvement of Tau in microfilaments stabilization through a cross-linking mechanism has been also identified [37]. Tau cleavage and/or change in its phosphorylation state are important early factors in the failure of the microtubule network that occurs during neuronal apoptosis [38, 39] or upon treatment with microtubules poisons commonly used in cancer therapy [40–42].

In this report, we aimed at characterizing the events upstream of cell cycle arrest and apoptosis triggered by DADS in neuroblastoma cells. Particularly, we found a superoxide-mediated disassembly of both microfilaments and microtubules concomitant to Tau dephosphorylation *via* PP1. Our results give efforts to the employ of DADS as a potent anti-neuroblastoma drug by virtue of its widespread cytoskeleton disrupting action on proliferating neuroblastoma cells.

Material and methods

Material

Diallyl disulphide, proteases inhibitor cocktail, NAC, GSH ester, mouse monoclonal anti-actin, anti- α - and anti- β -tubulin were from Sigma (St. Louis, MO, USA). Goat polyclonal anti-p-cdk5 and mouse monoclonal anti-Tau were from Santa Cruz Biotechnology (Santa Cruz, CA, USA). Mouse monoclonal anti-Tau-1 antibody (clone PC1C6) was from Millipore-Chemicon (Billerica, MA, USA). Rabbit polyclonal anti-p-Bcl-2 was from Cell Signalling Technology Inc. (Danvers, MA, USA). IgG (H+L)-HRP-conjugated secondary antibodies were from Bio-Rad Laboratories (Hercules, CA, USA). Anti-cleaved-Tau (TauC3) was a kind gift of Prof. Binder Lester I. (Dept. of Cell and Molecular Biology, Northwestern University, Feinberg School of Medicine, Chicago, IL, USA). Roscovitine, okadaic acid, zVADfmk, Calpain inhibitor II and JNK inhibitor I were from Calbiochem (Merck KGaA, Darmstadt, Germany). Alexa Fluor® 488-Phalloidin was from Invitrogen (Carlsbad, CA, USA). OxyBlot™ detection kit was from Chemicon (Temecula, CA, USA). All other chemicals were obtained from Merck (Darmstadt, Germany).

Cell cultures and treatments

SH-SY5Y and HeLa cells were purchased from the European Collection of Cell Cultures. hSOD cells were obtained by stably overexpressing SOD1 in SH-SY5Y cells as described previously [43]. SH-SY5Y and HeLa cells were grown in D-MEM-F12 and D-MEM, respectively, supplemented with 10% FCS, 1% penicillin/streptomycin and 1% glutamine (Lonza Ltd, Basel, Switzerland) and hSOD cells maintained in selection with 200 mg/ml G148. Cells were cultured at 37°C in an atmosphere of 5% CO₂ in air.

Fifty mM solution of DADS was prepared just before the experiments dissolving 5.5 M DADS in dimethyl sulfoxide (DMSO). DADS was used at concentration of 50 μ M up to 6 hrs unless otherwise stated. This concentration was selected as we previously demonstrated it was able to give valuable degree of cell cycle arrest and apoptosis at 12 hrs and 24 hrs, respectively, in SH-SY5Y cells [5, 6]. The cell permeable calpain inhibitor II (10 μ M), caspase-3 inhibitor zVADfmk (20 μ M), cdk5 inhibitor roscovitine (1 μ M), JNK inhibitor I (10 μ M), phosphatases inhibitor okadaic acid (5 or 50 nM) were dissolved in DMSO. NAC and GSH ester were dissolved in phosphate-buffered saline and used at concentration of 5 mM. Overall, these treatments were carried out 1 hr before the addition of DADS and maintained throughout the experiment. As controls, equal amounts of DMSO were added to untreated cells.

For differentiation, SH-SY5Y cells were treated for 5 days with 30 μ M retinoic acid, time that resulted in G1/G0 cell cycle arrest, acquisition of the morphology and up-regulation of proteins (such as GAP43) typical of differentiated cells.

Microscopy analysis

Cells were seeded directly on glass cover slips 24 hrs before DADS treatment. Cells were fixed with 4% paraformaldehyde and incubated with α -tubulin primary antibody (1:200). Successively, cells were incubated with the appropriate Alexa Fluor®568-conjugated secondary antibody (1:1000). F-actin was stained with Alexa Fluor® Phalloidin-488 (200 nM) and nuclei with Hoechst 33342 (10 μ g/ml). Then cover slips were fixed on microscope slides and digitized with a cool snap video camera connected to Nikon Eclipse TE200 epifluorescence microscopy (Nikon, Firenze, Italy). Alternatively, images were acquired on Olympus IX 70 equipped with Nanomover® and softWoRx DeltaVision (Applied Precision Inc., Issaquah, WA, USA) with a U-PLAN-APO 60 \times objective. Cell morphology was observed by light microscopy. All images were captured under constant exposure time, gain and offset.

SOD1 enzyme assay

SOD1 activity was measured on cell lysates by a polarographic method as reported previously [44]. Data were expressed as μ g/mg protein with reference to purified human Cu,Zn SOD.

Cell fractionation and Western blotting

Total cell lysates were obtained resuspending cell pellets in lysis buffer containing 10 mM Tris-HCl, pH 7.4, 5 mM EDTA, 150 mM NaCl, 0.5% IGEPAL CA-630, proteases and phosphatases inhibitors cocktail. The Triton-soluble cytosolic components were separated from the Triton-insol-

uble cytoskeletal components as previously described [45]. Protein content was determined according to Lowry *et al.* [46]. Protein extracts were resuspended in Laemmli Buffer and then electrophoresed on 10% or 12% SDS-polyacrylamide gels and blotted onto nitrocellulose. Membranes were stained with primary antibodies against actin (1:5000), α -tubulin (1:5000), β -tubulin (1:5000), p-cdk5 (1:2000), p-Bcl-2 (1:1000) or Tau (1:2000). Detection of cleaved Tau was carried out using a TauC3 monoclonal antibody according to Gamblin *et al.* [47], and 6-hr treatment with 0.5 μ M staurosporine was used for Tau cleavage positive control [39]. After incubation with the appropriate HRP-conjugated secondary antibodies (1:10000), protein bands were detected using a Fluorchem Imaging system upon incubation with ChemiGlow chemiluminescence substrate (Alpha Innotech, San Leandro, CA, USA). Density of immunoreactive bands was calculated using the software AlphaEaseFC and normalized for α -tubulin or Ponceau Red staining. For Ponceau Red normalization, we considered the density of the each entire lane obtained after staining of blotted nitrocellulose membrane.

Determination of protein carbonylation

For determination of protein carbonyls, cytoskeletal and cytosolic proteins were extracted according to Morris *et al.* [48]. Carbonylated proteins were detected using the OxyBlot™ Kit (Chemicon) according to the manufacturer's instruction. Briefly, 5 μ g of cytoskeletal proteins were reacted with 2,4-dinitrophenylhydrazine (DNP) for 15 min. at 25°C. Samples were resolved on 10% SDS-polyacrylamide gels and DNP-derivatized proteins were identified by Western blot analysis using an anti-DNP antibody and an appropriate HRP-conjugated secondary antibody.

Analysis of cell cycle and apoptosis

Cells were stained with 50 μ g/ml propidium iodide (dissolved in sodium citrate 1 mg/ml, 0.1% Triton X-100) prior cytofluorimetric analysis with FACScalibur instrument (Beckton & Dickinson, San José, CA, USA). The percentages of cells in G2/M phase and apoptotic cells were evaluated according to Nicoletti *et al.* [49] by using the WinMDI 2.8 software (the Scripps Research Institute, La Jolla, CA, USA).

Statistical analysis

The results are presented as means \pm S.D. Statistical evaluation was conducted by ANOVA, followed by the *post hoc* Student–Newman–Keuls. Differences were considered to be significant at $P < 0.05$.

Results

DADS induces cytoskeletal alterations in SH-SY5Y cells

Previously we demonstrated that DADS induces oxidative stress, cell cycle arrest and apoptosis in tumour cells of neuronal origin

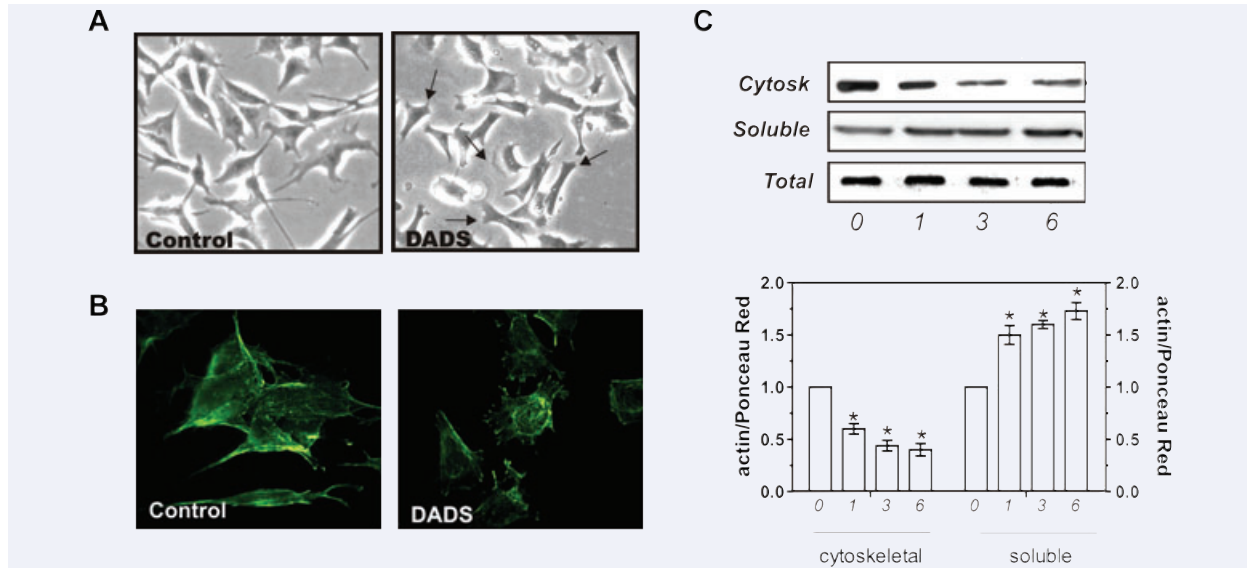


Fig. 1 DADS treatment induces alteration of cell morphology and microfilaments disruption in SH-SY5Y cells. **(A)** After 1-hr treatment with 50 μ M DADS, SH-SY5Y cells were fixed with paraformaldehyde and morphology was observed by light microscopy. **(B)** After 1-hr treatment with 50 μ M DADS, SH-SY5Y paraformaldehyde-fixed cells were incubated with AlexaFluor468-conjugated Phalloidin to stain F-actin and analysed by fluorescent microscope. Images reported are from one experiment representative of three that gave similar results. **(C)** SH-SY5Y cells were treated with 50 μ M DADS up to 6 hrs. At each time-point, cell pellets were used for separation of cytoskeletal and soluble or total proteins. Proteins were subjected to SDS-PAGE followed by Western blot analysis using an anti-actin antibody. Immunoblots reported are representative of four that gave similar results. Density of immunoreactive bands was measured by Quantity one software (Bio-Rad Laboratories). Data are expressed as means of actin/Ponceau Red \pm S.D.; $n = 4$, * $P < 0.001$.

via a ROS-mediated activation of JNK/c-Jun signalling pathway [5, 6]. In this report, we have focused on early effects of DADS treatment in order to characterize the molecular events upstream of induction of apoptosis in SH-SY5Y cells. We analysed cell morphology at early stages (during the first 6 hrs) after 50 μ M DADS administration, a concentration that efficiently triggers apoptosis at 24 hrs [6, 7]. As reported in Fig. 1A, control cells displayed the shape typical of SH-SY5Y neuroblastoma cells, whereas morphology of DADS-treated cells was altered starting from 1 hr with the number and extension of neurites significantly reduced. These variations preceded the blockage of cell cycle and induction of death, which was significant only after 12 hrs of DADS treatment [5].

To verify whether changes of cell morphology were associated with cytoskeleton alteration, we analysed microfilaments architecture after staining of actin stress fibres (F-actin) with Alexa Fluor 488-conjugated phalloidin. As reported in the panels of Fig. 1B, phalloidin staining confirmed the morphological changes observed in cells treated with DADS with respect to controls. Moreover, this analysis revealed that F-actin was considerably reduced starting at 1 hr (Fig. 1B). Western blot analysis carried out on cytoskeletal protein extracts evidenced that cytoskeletal actin was significantly reduced up to 6 hrs with a concomitant accumulation of its content in soluble fraction (Fig. 1C). Moreover, total actin protein content was not

altered confirming that a depolymerization process of microfilaments was occurring.

To deeply dissect the effects of DADS on cytoskeleton, we analysed both microtubules and microfilaments by an Olympus IX 70 equipped with Nanomover[®] and softWoRx DeltaVision fluorescent microscopy. Immunostaining of α -tubulin demonstrated that cells treated with DADS displayed a dramatic alteration of microtubules network contemporarily to F-actin loss (Fig. 2). In fact, while control cells displayed a well-defined microtubular organization, DADS-treated cells had a punctuated and disordered tubulin lattice. Nuclei staining with Hoechst 33342 also confirmed that cytoskeleton impairment occurred very early with respect to cell cycle blockage, as G2/M arrested cells were not still detected (data not shown). Figure 3A shows that DADS caused a significant decrease of β -tubulin in the cytoskeletal fraction starting at 3 hrs and a concomitant increase of the protein in the cytosolic counterpart, which reached the maximum level at 6 hrs, indicating a depolymerization process of microtubules. As seen for actin, total α -tubulin content was not altered (Fig. 3B). However, the occurrence of microtubules disruption was further confirmed by analysing the content of Bcl-2 protein phosphorylated on Ser70, which is widely considered a marker of microtubules depolymerization. Indeed, anti-microtubule agents (e.g. taxol, vincristine, vinblastine, nocodazole) can trigger Bcl-2 phosphorylation at G2/M phase of the cell cycle in a variety of human tumour cell

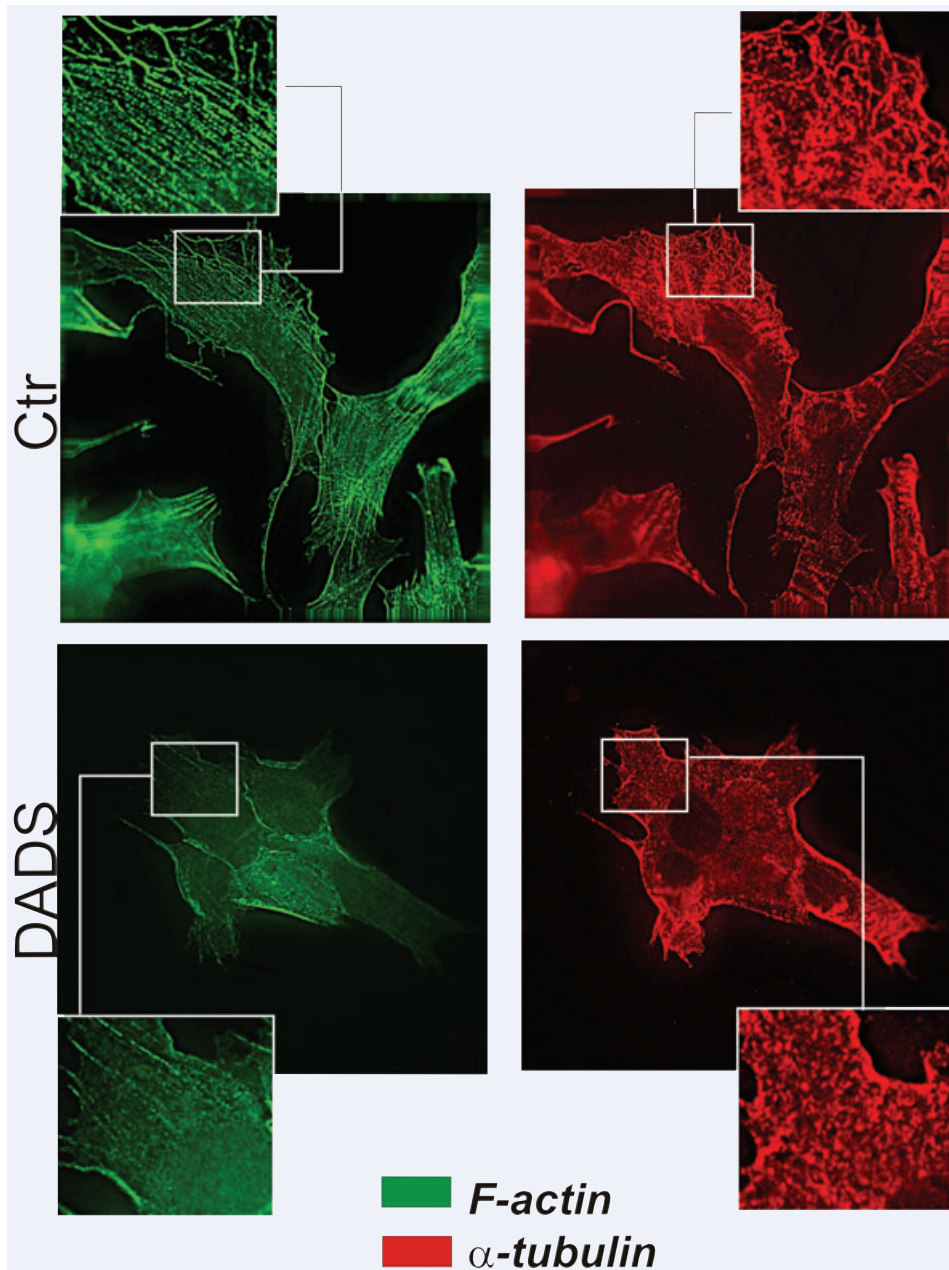


Fig. 2 DADS treatment alters microtubules network in SH-SY5Y cells. After 3-hr treatment with 50 μ M DADS, SH-SY5Y cells were fixed with paraformaldehyde and were incubated with AlexaFluor488-conjugated Phalloidin to stain F-actin (green), with an anti- α -tubulin and with the appropriate AlexaFluor568-conjugated secondary antibody to stain microtubules (red). Images reported are from one experiment representative of four that gave similar results.

lines [50, 51]. Western blot analysis, using an anti-phospho-Bcl-2 (p-Bcl-2) antibody specifically recognizing the phosphorylated Ser70, revealed that p-Bcl-2 increased time-dependently (Fig. 3B).

Superoxide is implicated in microfilaments and microtubules disruption

DADS is a pro-oxidant molecule able to rapidly increase intracellular ROS content and irreversibly damage cellular components

including membrane lipids, nucleus and proteins [5–7, 29]. We previously demonstrated that SH-SY5Y cells stably overexpressing SOD1 (hSOD cells) displayed increased superoxide dismutase activity with respect to SH-SY5Y cells ($2.80 \pm 0.12 \mu\text{g}/\text{mg prot}$ versus 0.95 ± 0.08) and efficiently counteracted both the ROS burst and the pro-apoptotic action of DADS [5]. In fact, as reported in Fig. 4A, a significant reduction of apoptotic cells was obtained at 24 hrs. Since cytoskeleton is considered one of the main targets of ROS, we asked whether hSOD cells could escape microfilaments- and/or microtubules-disrupting action of DADS.

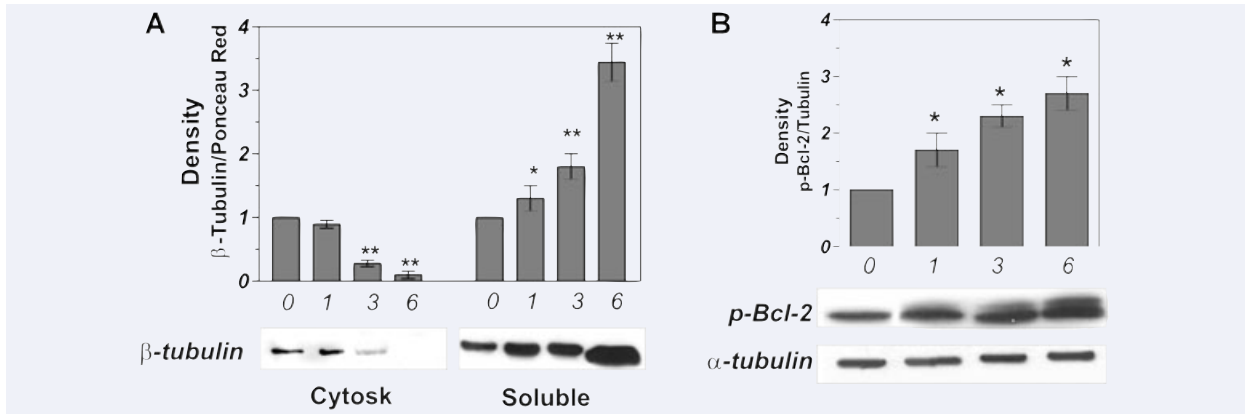


Fig. 3 DADS treatment induces microtubules depolymerization in SH-SY5Y cells. **(A)** SH-SY5Y cells were treated with 50 μ M DADS up to 6 hrs. At each time-point, cell pellets were used for separation of cytoskeletal and soluble proteins. Proteins were subjected to SDS-PAGE followed by Western blot analysis using an anti- β -tubulin antibody. Immunoblots reported are representative of four that gave similar results. Density of immunoreactive bands was measured by Quantity one software (Bio-Rad Laboratories). Ponceau Red protein staining on nitrocellulose membrane was used as loading control. Data are expressed as means of β -tubulin/Ponceau Red \pm S.D.; $n = 4$, * $P < 0.01$, ** $P < 0.001$. **(B)** SH-SY5Y cells were treated with 50 μ M DADS up to 6 hrs. At each time-point, cell pellets were used for total proteins extraction. Proteins were subjected to SDS-PAGE followed by Western blot analysis using an anti-p-Bcl-2 antibody. Anti- α -tubulin was used as loading control. Immunoblots reported are from one experiment representative of four that gave similar results. Density of immunoreactive bands was measured by Quantity one software (Bio-Rad Laboratories). Data are expressed as means of p-Bcl-2/ α -tubulin \pm S.D.; $n = 3$, * $P < 0.001$.

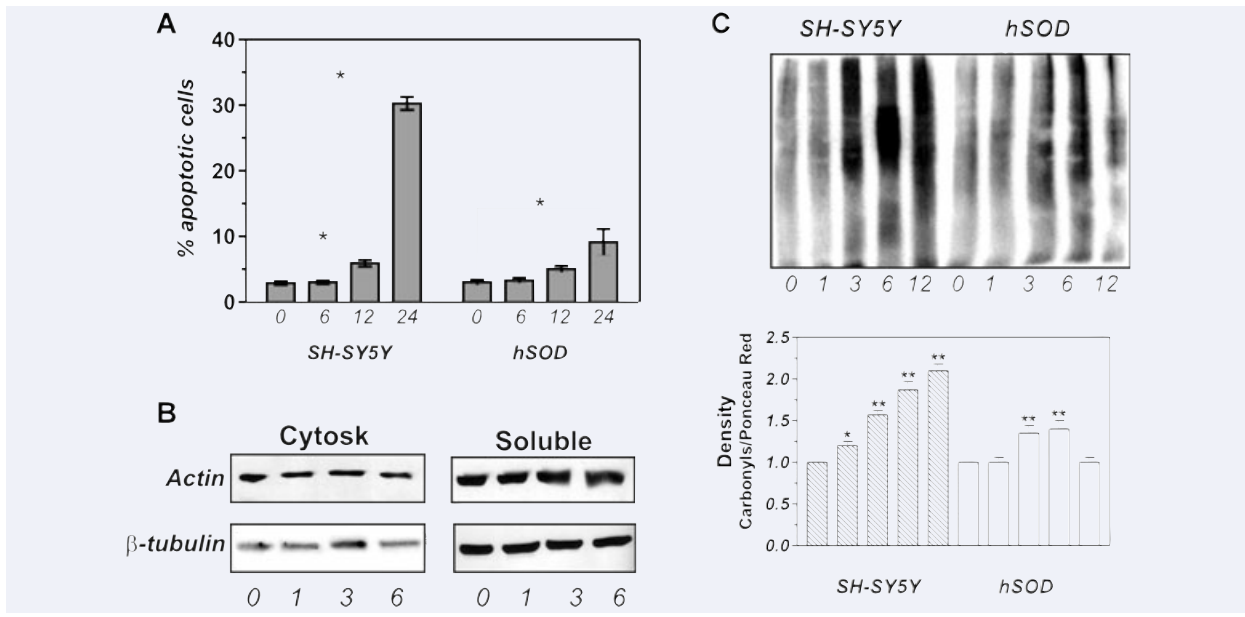


Fig. 4 SOD1 overexpression protects SH-SY5Y from cytoskeletal disruption. **(A)** SH-SY5Y and hSOD cells were treated with 50 μ M DADS for the indicated times. Cytofluorimetric analysis of apoptosis was carried out after staining of nuclei with propidium iodide. Data are expressed as means \pm S.D.; $n = 8$, * $P < 0.001$. **(B)** hSOD cells were treated with 50 μ M DADS up to 6 hrs. At each time-point, cell pellets were used for separation of cytoskeletal and soluble proteins. Proteins were subjected to SDS-PAGE followed by Western blot analysis using an anti- β -tubulin or anti-actin antibody. Immunoblots reported are from one experiment representative of four that gave similar results. **(C)** SH-SY5Y and hSOD cells were treated with 50 μ M DADS up to 12 hrs. At each time-point, cell pellets were used for separation of cytoskeletal or soluble proteins. Protein carbonyls were derivatized with DNP and subjected to SDS-PAGE followed by Western blot analysis using an anti-DNP antibody. Immunoblot reported is representative of four that gave similar results. Density of immunoreactive bands was measured by Quantity one software (Bio-Rad Laboratories). Ponceau Red protein staining on nitrocellulose membrane was used as loading control. Data are expressed as means of protein carbonyls/Ponceau Red \pm S.D.; $n = 4$, * $P < 0.01$, ** $P < 0.001$.

Western blot analysis of actin and β -tubulin on soluble and cytoskeletal fractions evidenced that the content of these proteins was not altered in hSOD cells treated with DADS (Fig. 4B).

These results suggested that cytoskeleton disassembly could depend on superoxide-mediated oxidative modifications of its protein constituents. To verify this hypothesis, we measured the level of carbonyl residues in cytoskeletal protein extracts. After derivatization of carbonyls with DNP, cytoskeletal protein extracts from either SH-SY5Y or hSOD cells were subjected to Western blot analysis using an anti-DNP antibody. As reported in Fig. 4C, cytoskeletal proteins of SH-SY5Y cells were oxidatively damaged as early as after 1 hr reaching a peak level at 12 hrs. On the contrary, cytoskeletal proteins of hSOD cells were faintly carbonylated only at 3 and 6 hrs to finally return to the basal level at 12 hrs after DADS administration.

DADS induces PP1-mediated Tau dephosphorylation

On the basis of the results obtained on cytoskeletal disassembly, we asked whether Tau could be affected in the early hours after DADS administration. To this end, we analysed Tau protein by Western blot analysis using an antibody directed against all Tau isoforms and recognizing it independently on its phosphorylation state. As showed in Fig. 5A, the monoclonal antibody recognized a major Tau band and a faint band at higher molecular weight. DADS treatment caused an early shift of the bands towards lower molecular weights, which remained constant for all the time-points screened. The appearance of low molecular weight forms of Tau has been frequently ascribed to many factors including dephosphorylation, calpains- or caspases-mediated cleavage [39, 52]. We therefore investigated the possible involvement of calpains and caspases in Tau processing by treating SH-SY5Y cells with chemical inhibitors of these two proteases, specifically 20 μ M z-VAD_{FMK} and 10 μ M calpain inhibitor II. As evidenced in the immunoblot reported in Fig. 5B, none of the two inhibitors used were able to reconstitute the control Tau pattern. To confirm this result, cell lysates were also used for Western blot analysis using an antibody specific for the caspases-cleaved form of Tau. As positive control, we treated cells with the pro-apoptotic agent staurosporine, which efficiently induces Tau processing by caspase-3 during neuronal apoptosis [39]. As showed in immunoblot reported in Fig. 5C, this analysis revealed that Tau was not cleaved during DADS treatment, whereas a strong Tau-cleaved immunoreactive band was observed in cells treated with staurosporine. We then attempted to explore whether Tau could be dephosphorylated by the action of protein phosphatase-1 and/or -2A (PP1 and PP2A), which have been identified as the principal phosphatases modulating Tau phosphorylation state also in SH-SY5Y cells [53, 54]. We therefore co-treated cells with okadaic acid (OA), a strong inhibitor of both PP1 and PP2A in dependence of its concentration. Western blot analysis of Tau showed that PP2A was not involved in Tau dephosphorylation as no significant changes were detected in cells treated with DADS or

in combination with 5 nM OA (Fig. 5D), concentration exclusively inhibiting PP2A. Instead, concomitant inhibition of PP1 and PP2A by treatment with 50 nM OA completely abolished the appearance of the lower molecular weight bands observed with DADS treatment alone (Fig. 5D), suggesting that they likely corresponded to dephosphorylated Tau forms and that a DADS-mediated activation of PP1 occurred. To confirm this hypothesis, we carried out Western blot analysis also with Tau-1 antibody, which specifically recognizes only the dephosphorylated forms of Tau. Figure 5E shows that after DADS treatment Tau dephosphorylated bands increased in number and immunoreactivity.

DADS-mediated ROS increase is responsible for Tau dephosphorylation

It has been established that PP1 is activated by oxidative stress leading to dephosphorylation of its substrates including Tau [55–57]. Indeed, PP1 can be activated directly by H₂O₂ [58] or by the redox-mediated dissociation of its inhibitory partners [59]. The latter is a regulatory mechanism that mainly involves the binding of the inhibitor protein 2 (I-2), which can be reversed under oxidative stimuli by cdk5-mediated phosphorylation of I-2 [57, 60]. To assess whether cdk5 could be involved in the signalling pathway converging to Tau dephosphorylation, we carried out Western blot analysis of phospho-active cdk5 (p-cdk5). Figure 6A shows that DADS treatment was not associated with the induction of cdk5 phosphorylation, indicating that this kinase was not involved. Moreover, experiments carried out in the presence of the cdk5 inhibitor roscovitine demonstrated that Tau dephosphorylation was not prevented (Fig. 6B), thus excluding the influence of cdk5 on Tau phosphorylation in our experimental model. We then investigated whether JNK, which is strongly activated following DADS treatment [5], could be the up-stream mediator of tau dephosphorylation. Experiments carried out in the presence of the synthetic inhibitor of JNK (JNK inhibitor I) demonstrated that it did not prevent tau dephosphorylation (Fig. 6B). On the basis of these results, we attempted to analyse the possible direct participation of ROS on the route leading to Tau dephosphorylation. To test this hypothesis, we examined Tau in hSOD cells: contrarily to microtubules and microfilaments, SOD1 overexpression had no inhibitory effects on Tau dephosphorylation (Fig. 6C), implying that superoxide could not mediate this event. To assess whether H₂O₂ could be involved, we pre-treated cells with two-electron reductants such as NAC or GSH-ester prior to DADS administration and we subsequently analysed Tau by Western blot. As showed in immunoblot reported in Fig. 6D, both antioxidants were able to efficiently prevent Tau dephosphorylation. Concomitantly, NAC pre-treatment completely abolished DADS disrupting action both on microtubules and microfilaments (Fig. 7A). As reported in Fig. 7B, cytofluorimetric analysis upon propidium iodide staining revealed that NAC was also able to completely prevent both G2/M growth arrest and apoptosis.

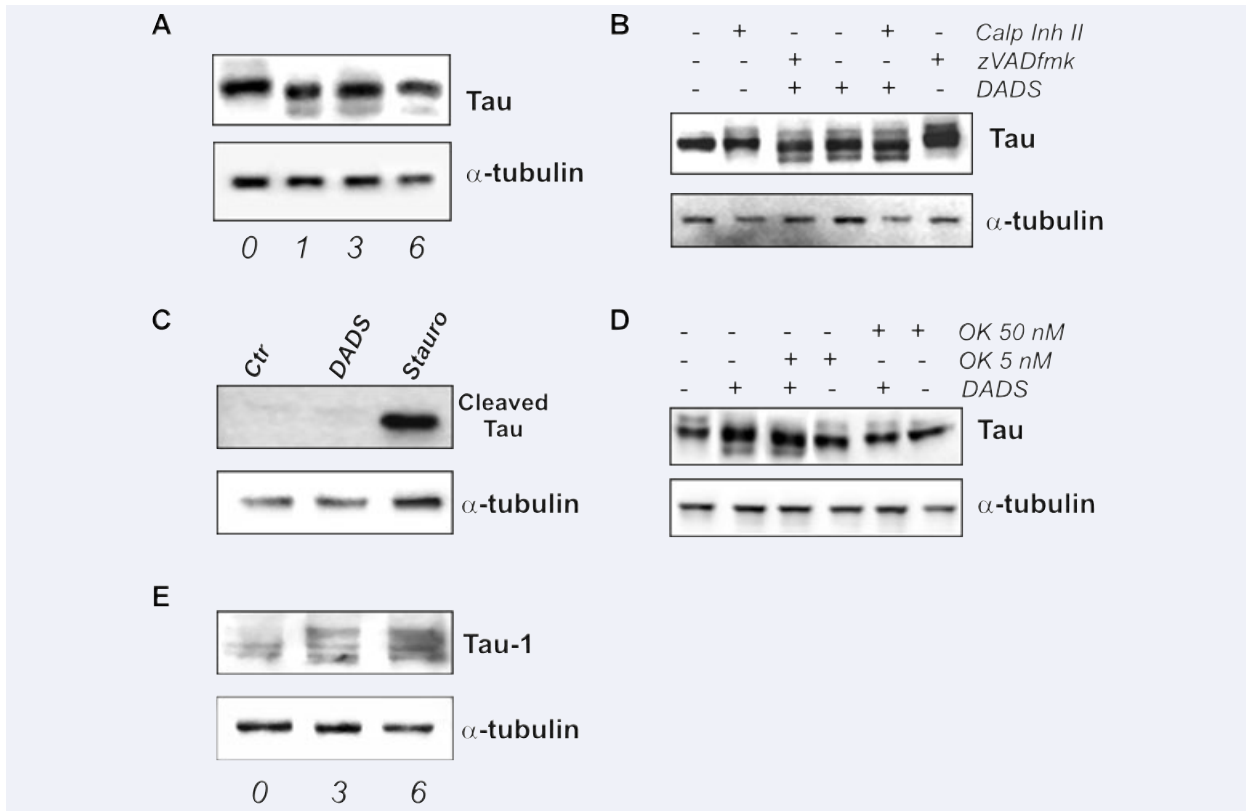


Fig. 5 DADS induces PP1-mediated Tau dephosphorylation. **(A)** SH-SY5Y cells were treated with 50 μ M DADS up to 6 hrs. At each time-point, cell pellets were lysed and total protein extracts were subjected to SDS-PAGE followed by Western blot analysis using an anti-Tau antibody recognizing Tau protein independently of its phosphorylation state and anti- α -tubulin antibody as loading control. Immunoblots reported are from one experiment representative of four that gave similar results. **(B)** One hour before 50 μ M DADS treatment, caspase 3 inhibitor (zVADfmk) or calpain inhibitor II was added to culture medium and maintained throughout the experiment. After 3 hrs, cell pellets were lysed and total protein extracts were subjected to SDS-PAGE followed by Western blot analysis using an anti-Tau antibody recognizing Tau protein independently on its phosphorylation state and anti- α -tubulin antibody as loading control. Immunoblots reported are from one experiment representative of four that gave similar results. **(C)** SH-SY5Y cells were treated with 50 μ M DADS for 6 hrs. Cell pellets were lysed and total protein extracts were subjected to SDS-PAGE followed by Western blot analysis using an anti-TauC3 antibody recognizing only its caspase 3-cleaved form and anti- α -tubulin antibody as loading control. Six-hour treatment with 0.5 μ M staurosporine was used as positive control. Immunoblots reported are from one experiment representative of three that gave similar results. **(D)** One hour before 50 μ M DADS treatment, okadaic acid (OA) was added to culture medium and maintained throughout the experiment. After 3 hrs, cell pellets were lysed and total protein extracts were subjected to SDS-PAGE followed by Western blot analysis using an anti-Tau antibody recognizing Tau protein independently on its phosphorylation state and anti- α -tubulin antibody as loading control. Immunoblots reported are from one experiment representative of three that gave similar results. **(E)** SH-SY5Y cells were treated with 50 μ M DADS up to 6 hrs. At each time-point, cell pellets were lysed and total protein extracts were subjected to SDS-PAGE followed by Western blot analysis using an anti-Tau1 antibody recognizing only Tau dephosphorylated forms and anti- α -tubulin antibody as loading control. Immunoblots reported are from one experiment representative of three that gave similar results.

HeLa cells, which do not have cytoskeletal-associated Tau protein, were treated with the same concentration of DADS. Figure 7C shows that these cells are less susceptible to DADS toxicity indicating that Tau could play a synergistic role in apoptosis commitment.

We previously demonstrated that differentiated SH-SY5Y cells were not committed to apoptosis by DADS treatment [6]. Therefore, we analysed the effects of DADS on cytoskeleton network of SH-SY5Y differentiated with retinoic acid. We found that these cells were still sensitive to anti-cytoskeleton action of DADS as they underwent both microfilaments/microtubules disruption

and Tau dephosphorylation (data not shown), indicating that cytoskeletal disrupting action of DADS could be more detrimental for proliferating cells.

Discussion

Anti-cancer drugs interfering with cytoskeletal dynamics are currently employed in chemotherapy and the most successful in

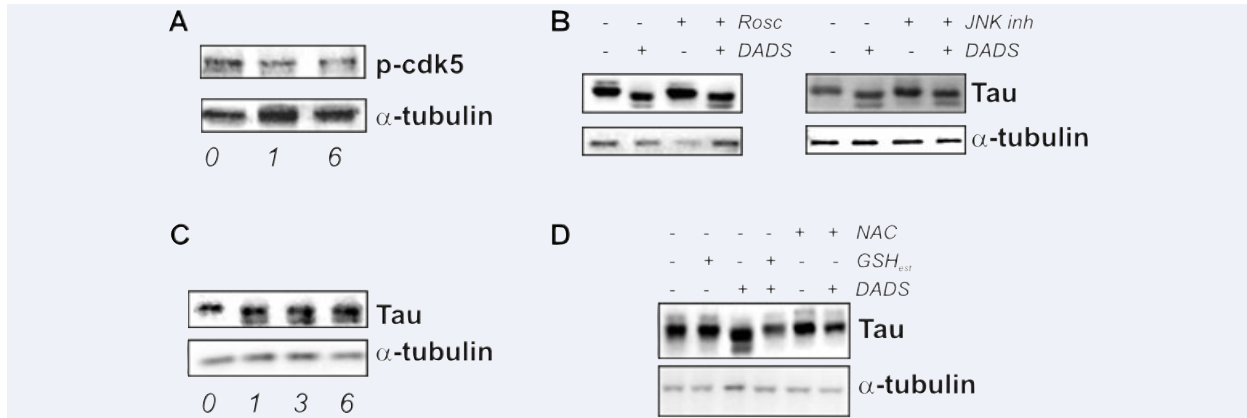


Fig. 6 Tau dephosphorylation is mediated by H₂O₂ and is prevented by NAC and GSH_{est}. **(A)** SH-SY5Y cells were treated with 50 μ M DADS. At indicated times, cells were lysed and total protein extracts were subjected to SDS-PAGE followed by Western blot analysis using an anti-p-cdk5 antibody and anti- α -tubulin antibody as loading control. Immunoblots reported are from one experiment representative of three that gave similar results. **(B)** One hour before 50 μ M DADS treatment, 1 μ M roscovitin (*Rosc*) or JNK inhibitor I (*JNK inh*) was added to culture medium and maintained throughout the experiment. After 3 hrs, cell pellets were lysed and total protein extracts were subjected to SDS-PAGE followed by Western blot analysis using an anti-Tau antibody recognizing Tau protein independently on its phosphorylation state and anti- α -tubulin antibody as loading control. Immunoblots reported are from one experiment representative of three that gave similar results. **(C)** Cu,Zn SOD overexpressing cells (hSOD) were treated with 50 μ M DADS up to 6 hrs. At each time-point, cell pellets were lysed and total protein extracts were subjected to SDS-PAGE followed by Western blot analysis using an anti-Tau antibody recognizing Tau protein independently on its phosphorylation state and anti- α -tubulin antibody as loading control. Immunoblots reported are from one experiment representative of four that gave similar results. **(D)** One hour before 50 μ M DADS treatment, 5 mM NAC or 5 mM GSH_{est} was added to culture medium and maintained throughout the experiment. After 3 hrs, cell pellets were lysed and total protein extracts were subjected to SDS-PAGE followed by Western blot analysis using an anti-Tau antibody recognizing Tau protein independently on its phosphorylation state and anti- α -tubulin antibody as loading control. Immunoblots reported are from one experiment representative of three that gave similar results.

inhibiting proliferation without affecting cytoskeleton of normal cells are those targeting microtubules and impeding mitotic spindle assembly [28]. As previously suggested, some organosulphur garlic compounds including DADS exert anti-mitotic effects that nicely resembles those of the most used anti-microtubules agents such as nocodazole and *Vinca* alkaloids [30–33, 61]. The unique proposed mechanism of action is microtubules oxidation by direct binding on tubulin at alternative sites with respect to the above-mentioned drugs. In particular, adducts between the organosulphur compound and tubulin cysteine thiols have been suggested to be formed since sulphhydryls-reducing agents (dithiothreitol and β -mercaptoethanol) abolish the disrupting effect on microtubules. The subsequent identification of an allylmercaptocysteine adducts on Cys¹² and Cys³⁵⁴ of β -tubulin gave the ultimate demonstration of the fundamental role of allyl moiety in causing mitotic arrest through microtubules oxidation and destabilization [32]. Our results are in line with the notion that DADS causes impairment of microtubules as we detected a significant loss of microtubules network together with a rapid and abnormal accumulation of soluble β -tubulin with the cytoskeletal counterpart being concomitantly reduced. Disassembly activity of DADS on microtubules was also confirmed by analysing phosphorylation of Bcl-2 on Ser70, which is generally considered a marker of microtubules impairment [50, 51]. p-Bcl-2 increased irrespective of total decrement of non-phosphorylated Bcl-2, which we previously detected at early

times after DADS administration, indicating a strong anti-microtubules activity of DADS. By the use of SOD1 overexpressing cells we demonstrated that microtubules disassembly could be triggered only in the presence of superoxide. Indeed, SH-SY5Y cells underwent oxidative modifications of cytoskeletal proteins and hSOD cells were highly protected both from carbonylation and from microtubules depolymerization. These data nicely correlate with those previously obtained in our laboratory, which showed carbonylation in total protein extracts of SH-SY5Y cells [5], indicating that carbonylation of cytoskeletal proteins has a significant contribute in the raise of total protein carbonyls. Our results do not exclude that the allylation of β -tubulin also occurs but rather they imply that DADS-derived superoxide, besides causing oxidative damage through carbonylation, was somehow necessary to allow the reaction of allyl moiety with β -tubulin thiols.

While the occurrence of microtubules depolymerization upon treatment with allyl-containing garlic derivatives was already suggested by other authors, the present work gives the first evidence of microfilaments disruption. Like microtubules, microfilaments can undergo oxidative modifications both on methionine and cysteine of actin upon treatment with oxidizing agents [8, 9, 62]. It was therefore plausible that the oxidative action of DADS could affect also microfilament network. However, to the best of our knowledge, only the effects of allicin on microfilaments have been explored with conflicting results. In fact, Prager-Khoutorsky and

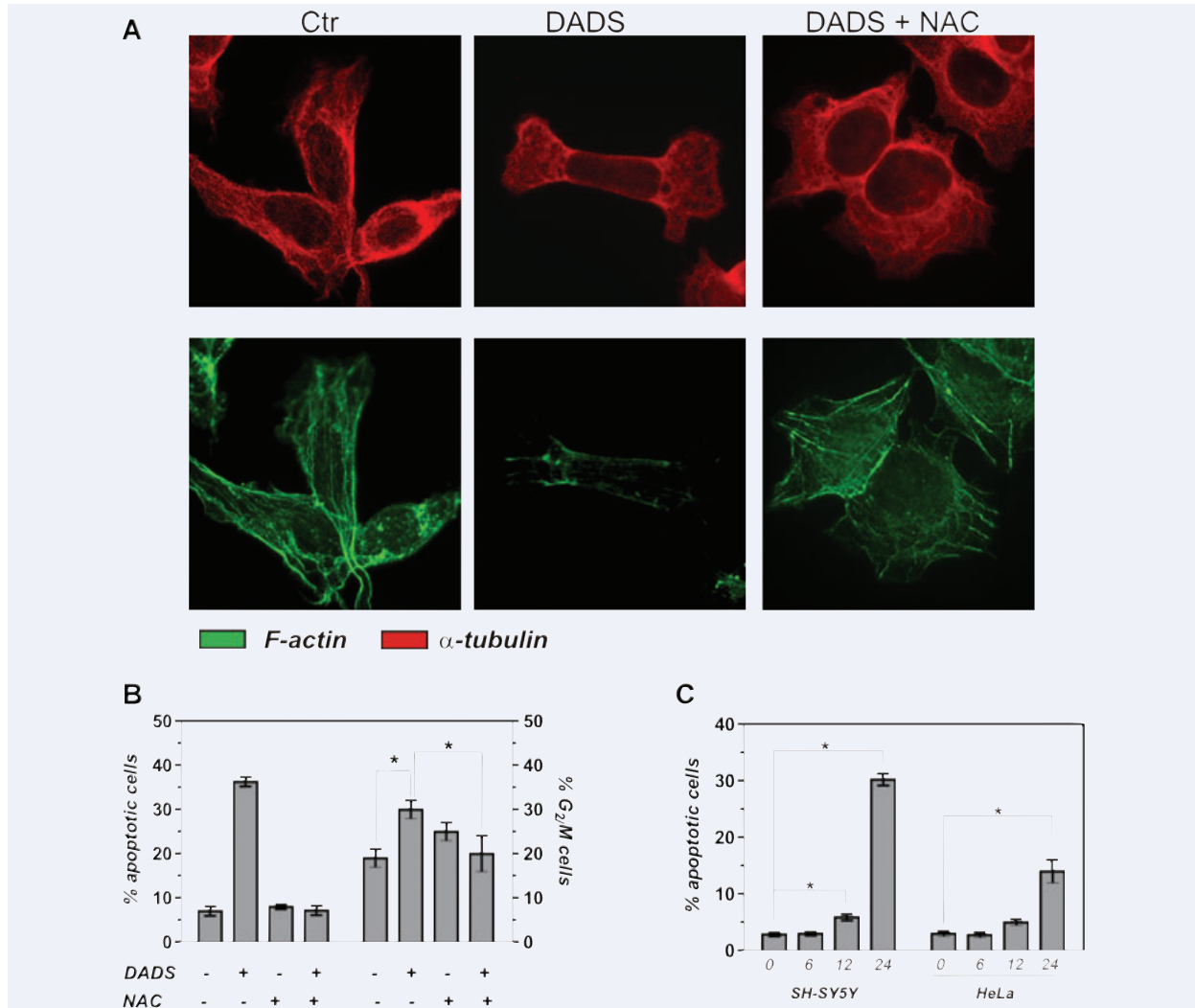


Fig. 7 NAC protects from DADS-induced cytoskeleton disruption and apoptosis. **(A)** One hour before 50 μ M DADS treatment, 5 mM NAC was added to culture medium and maintained throughout the experiment. After 3-hr treatment with 50 μ M DADS, SY-SY5Y cells were fixed with paraformaldehyde and incubated with AlexaFluor488-conjugated Phalloidin to stain F-actin (green) and with an anti- α -tubulin to stain microtubules (red). After incubation with the appropriate AlexaFluor568-conjugated secondary antibody, cells were observed by fluorescent microscope. Images reported are from one experiment representative of three that gave similar results. **(B)** One hour before 24-hr treatment with 50 μ M DADS, 5 mM NAC was added to culture medium and maintained throughout the experiment. Cytofluorimetric analysis of apoptosis and cell cycle phases were carried out after staining of nuclei with propidium iodide. Data are expressed as means \pm S.D.; $n = 8$, $*P < 0.001$. **(C)** HeLa cells were treated with 50 μ M DADS for 24 hrs. Cytofluorimetric analysis of apoptosis was carried out after staining of nuclei with propidium iodide. Data are expressed as means \pm S.D.; $n = 4$, $*P < 0.001$.

co-workers reported that allicin treatment did not cause alteration of F-actin in fibroblast, while the group of Sela stated that allicin interfered with the reorganization of cortical actin impairing T cells motility [33, 35]. The appearance of carbonylated proteins in cytoskeletal fraction with broad molecular weight range strongly supported that a general oxidation process occurred inside cytoskeleton of DADS-treated cells, which was not limited to tubulin. Actually, the results on microfilaments were comparable

to those obtained on microtubules as demonstrated by the overlapping kinetics of actin and tubulin decrement in cytoskeletal fraction and their accumulation in the non-polymerized counterpart. Similarly, upon SOD1 overexpression, DADS failed in inducing microfilaments alteration. Thus, we suggest that DADS-derived superoxide actively participates in both actin and tubulin oxidation ultimately contributing to microfilaments and microtubules disruption.

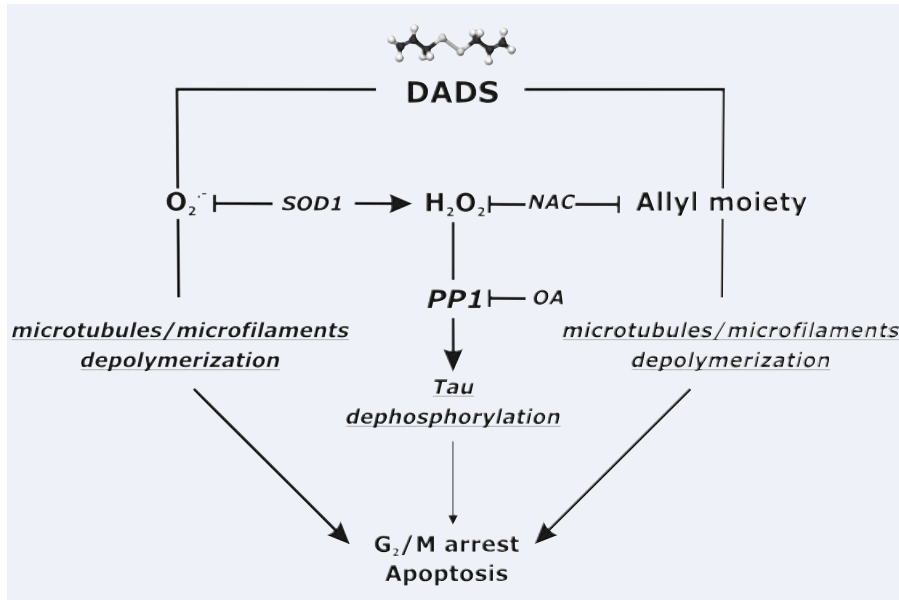


Fig. 8 Schematic model of the anti-cytoskeleton action of DADS. Tau dephosphorylation is likely caused by H_2O_2 -mediated activation of PP1. Both OA and NAC treatments prevent Tau dephosphorylation by inhibiting PP1 and scavenging H_2O_2 , respectively. Microfilaments and microtubules architecture is impaired by superoxide and allyl moiety and is preserved both by SOD1 and NAC. Tau dephosphorylation and microfilaments/microtubules depolymerization are two independent phenomena that differently contribute to G₂/M arrest and apoptosis commitment. The latter event appears to give the more relevant contribution to the anti-proliferative effects of DADS. DADS: diallyl disulphide; PP1: protein phosphatase 1; OA: okadaic acid; SOD1: copper,zinc superoxide dismutase; NAC: N-acetyl-L-cysteine.

Another unexplored event that we evidenced was the capacity of DADS to affect Tau state. This microtubules-associated protein is largely expressed in neurons and is involved in assembly and stabilization of microtubules [36, 63]. Tau function is regulated by a serine/threonine phosphorylation mechanism involving the concerted activity of specific kinases and phosphatases [59, 64]. Abnormal accumulation of hyperphosphorylated and dephosphorylated forms of Tau are associated with several tauopathies and neuronal apoptosis, respectively [25, 38, 39, 64]. It has been demonstrated that microtubules disassembly is necessary for Tau dephosphorylation to occur and this event precedes the apoptosis execution phase [65]. The results obtained from hSOD cells indicate that Tau dephosphorylation and microfilaments/microtubules disruption could be unlinked phenomena. During apoptosis, Tau can undergo caspases- or calpains-mediated cleavage [38, 47]. In our experimental model, the alteration of Tau pattern was not due to its cleavage either by caspase-3 or by calpains inhibitors. In addition, the time in which Tau state is altered did not coincide with that of caspase-3 activation, which became significant only later [5]. Our results strongly indicate that Tau was dephosphorylated, as demonstrated by the use of Tau-1 antibody specifically recognizing only its dephosphorylated forms. Moreover, this event occurs by a mechanism involving PP1 activation. Indeed, when we pre-incubated the cells with OA, at concentration inhibiting PP1, Tau phosphorylation pattern was not affected by DADS.

PP1 is a serine/threonine phosphatase having several protein substrates including phosphorylated Tau [64]. PP1 is regulated by multiple mechanisms among which the interaction with inhibitor subunits is the most characterized [59]. The concept that PP1 activity can be modulated in a redox-dependent manner is gradually emerging. It has been recently demonstrated that, upon oxidative insult, PP1 activity is stimulated after detachment of the

inhibitor I-2 through the cdk5 redox-dependent pathway. Likewise, oxidative burst allows activating PP1 to dephosphorylate Tau [57]. Although ROS production was early enhanced upon DADS treatment in SH-SY5Y cells [5], an increase of cdk5 phospho-active form was not found and the selective cdk5 inhibitor roscovitine did not impede alteration of Tau state, excluding the involvement of p35/cdk5 pathway in this process. The experiments carried out with the JNK inhibitor demonstrated that this kinase did not participate in the route leading to Tau dephosphorylation. Conversely, our results sustain the idea that Tau dephosphorylation could be triggered by the direct action of ROS on PP1. Particularly, H_2O_2 seems to be the species mainly causing Tau dephosphorylation. Actually, we found that in SH-SY5Y cells Tau can be dephosphorylated by H_2O_2 treatment but not by the superoxide-generating agents paraquat and rotenone (data not shown). Here we show that overexpression of SOD1 did not prevent DADS-mediated Tau dephosphorylation, indicating that superoxide is not involved in this process. Our hypothesis is supported by the data reported by Sommer *et al.*, who demonstrated that purified PP1 is significantly activated by H_2O_2 but not by superoxide [58]. The idea that Tau alteration is an H_2O_2 -mediated process is also confirmed by results obtained in the presence of the more general ROS scavengers NAC and GSH-ester, which completely abolished Tau dephosphorylation. NAC was also the most efficient agent able to completely impede early microfilaments/microtubules disassembly and counteract G₂/M arrest and apoptosis. This confirms that cytoskeletal filaments integrity can be preserved not only by scavenging superoxide through SOD1, but also by maintaining the reduced cytoskeletal proteins thiols as suggested for NAC by Hosono and co-workers [34]. The full capacity of NAC to preserve DADS-treated cells could therefore be the results of its double action on microfilaments/microtubules and Tau. The results

obtained suggest that G2/M arrest and apoptosis can be mostly prevented through blockage of cytoskeletal filaments depolymerization (*e.g.* by SOD1 overexpression or by NAC treatment) and that Tau more marginally participate in apoptosis commitment. In fact, hSOD cells display a non-complete protection against DADS-induced apoptosis that can be accounted for the occurrence of Tau dephosphorylation. Moreover, we found that inhibition of PP1 significantly decrease apoptotic cell death (data not shown) implying that Tau dephosphorylation and PP1 could contribute to DADS-mediated cytotoxicity.

Moreover, we show that HeLa cells, which do not express cytoskeletal Tau, are more resistant to DADS-mediated apoptosis, reinforcing the hypothesis for a synergistic role of Tau in the induction of cell death in tumour cells of neuronal origin.

A plausible schematic model of the anti-cytoskeleton action of DADS is presented in Fig. 8.

As both microtubules and actin filaments play important roles in mitosis, cell signalling and motility of proliferating cells, these cytoskeletal filaments are the targets of a growing number of anti-cancer drugs. However, only anti-microtubules agents have been successfully employed in cancer management as microfilaments poisons display high cytotoxicity for non-cancerous cells as well. Even if less significant with respect to undifferentiated

cells, also retinoic acid-treated SH-SY5Y cells underwent cytoskeleton depolymerization and Tau dephosphorylation (data not shown). However, regardless of the cytoskeleton alteration, they were completely resistant to DADS-mediated apoptosis [6], demonstrating that cytoskeleton impairment is lethal only for proliferating cells. Our results give emphasis to the possible employment of DADS in cancer treatment both by virtue of its widespread cytoskeletal alteration and specific cytotoxic action on proliferating neuroblastoma cells. Since neuronal cytoskeleton function highly depends on the phosphorylative status of Tau, the present work highlights Tau as a novel target of DADS anti-cytoskeleton action that can be also exploited for developing new strategy for treatment of neuronal pathologies associated with Tau hyperphosphorylation and phosphatases activity impairment (*i.e.* tauopathies).

Acknowledgements

We gratefully acknowledge Palma Mattioli for her assistance in microscopy and image analysis. This work was partially supported by grants from Ministero della Salute and MIUR, FIRB 'Idee Progettuali'.

References

1. **Shukla Y, Kalra N.** Cancer chemoprevention with garlic and its constituents. *Cancer Lett.* 2007; 247: 167–81.
2. **Rahman K, Lowe GM.** Garlic and cardiovascular disease: a critical review. *J Nutr.* 2006; 136: 736S–40S.
3. **Block E.** The chemistry of garlic and onions. *Sci Am.* 1985; 252: 114–9.
4. **Herman-Antosiewicz A, Powolny AA, Singh SV.** Molecular targets of cancer chemoprevention by garlic-derived organosulfides. *Acta Pharmacol Sin.* 2007; 28: 1355–64.
5. **Filomeni G, Aquilano K, Rotilio G, et al.** Reactive oxygen species-dependent c-Jun NH2-terminal kinase/c-Jun signaling cascade mediates neuroblastoma cell death induced by diallyl disulfide. *Cancer Res.* 2003; 63: 5940–9.
6. **Aquilano K, Filomeni G, Baldelli S, et al.** Neuronal nitric oxide synthase protects neuroblastoma cells from oxidative stress mediated by garlic derivatives. *J Neurochem.* 2007; 101: 1327–37.
7. **Filomeni G, Aquilano K, Rotilio G, et al.** Glutathione-related systems and modulation of extracellular signal-regulated kinases are involved in the resistance of AGS adenocarcinoma gastric cells to diallyl disulfide-induced apoptosis. *Cancer Res.* 2005; 65: 11735–42.
8. **Dalle-Donne I, Rossi R, Milzani A, et al.** The actin cytoskeleton response to oxidants: from small heat shock protein phosphorylation to changes in the redox state of actin itself. *Free Radic Biol Med.* 2001; 31: 1624–32.
9. **Dalle-Donne I, Rossi R, Giustarini D, et al.** Methionine oxidation as a major cause of the functional impairment of oxidized actin. *Free Radic Biol Med.* 2002; 32: 927–37.
10. **Kang KW, Lee SJ, Kim SG.** Molecular mechanism of nrf2 activation by oxidative stress. *Antioxid Redox Signal.* 2005; 7: 1664–73.
11. **Boutte AM, Woltjer RL, Zimmerman LJ, et al.** Selectively increased oxidative modifications mapped to detergent-insoluble forms of Abeta and beta-III tubulin in Alzheimer's disease. *FASEB J.* 2006; 20: 1473–83.
12. **Mirabelli F, Salis A, Perotti M, et al.** Alterations of surface morphology caused by the metabolism of menadione in mammalian cells are associated with the oxidation of critical sulfhydryl groups in cytoskeletal proteins. *Biochem Pharmacol.* 1988; 37: 3423–7.
13. **Rokutan K, Johnston RB Jr, Kawai K.** Oxidative stress induces S-thiolation of specific proteins in cultured gastric mucosal cells. *Am J Physiol.* 1994; 266: G247–54.
14. **Caprari P, Bozzi A, Malorni W, et al.** Junctional sites of erythrocyte skeletal proteins are specific targets of tert-butylhydroperoxide oxidative damage. *Chem Biol Interact.* 1995; 94: 243–58.
15. **Banan A, Zhang Y, Losurdo J, et al.** Carbonylation and disassembly of the F-actin cytoskeleton in oxidant induced barrier dysfunction and its prevention by epidermal growth factor and transforming growth factor alpha in a human colonic cell line. *Gut.* 2000; 46: 830–7.
16. **Dourdin N, Bhatt AK, Dutt P, et al.** Reduced cell migration and disruption of the actin cytoskeleton in calpain-deficient embryonic fibroblasts. *J Biol Chem.* 2001; 276: 48382–8.
17. **van Engeland M, Kuijpers HJ, Ramaekers FC, et al.** Plasma membrane alterations and cytoskeletal changes in apoptosis. *Exp Cell Res.* 1997; 235: 421–30.
18. **Sanchez-Alcazar JA, Rodriguez-Hernandez A, Cordero MD, et al.** The apoptotic microtubule network preserves plasma membrane integrity during the execution phase of apoptosis. *Apoptosis.* 2007; 12: 1195–208.

19. **Brown SB, Bailey K, Savill J.** Actin is cleaved during constitutive apoptosis. *Biochem J.* 1997; 323: 233–7.
20. **Mashima T, Naito M, Tsuruo T.** Caspase-mediated cleavage of cytoskeletal actin plays a positive role in the process of morphological apoptosis. *Oncogene.* 1999; 18: 2423–30.
21. **Marceau N, Schutte B, Gilbert S, et al.** Dual roles of intermediate filaments in apoptosis. *Exp Cell Res.* 2007; 313: 2265–81.
22. **Lei K, Davis RJ.** JNK phosphorylation of Bim-related members of the Bcl2 family induces Bax-dependent apoptosis. *Proc Natl Acad Sci USA.* 2003; 100: 2432–7.
23. **Kensler TW, Wakabayashi N, Biswal S.** Cell survival responses to environmental stresses via the Keap1-Nrf2-ARE pathway. *Annu Rev Pharmacol Toxicol.* 2007; 47: 89–116.
24. **Woodring PJ, Hunter T, Wang JY.** Regulation of F-actin-dependent processes by the Abl family of tyrosine kinases. *J Cell Sci.* 2003; 116: 2613–26.
25. **Lee VM, Goedert M, Trojanowski JQ.** Neurodegenerative tauopathies. *Annu Rev Neurosci.* 2001; 24: 1121–59.
26. **Jordan MA, Wilson L.** Microtubules and actin filaments: dynamic targets for cancer chemotherapy. *Curr Opin Cell Biol.* 1998; 10: 123–30.
27. **Zhou J, Giannakakou P.** Targeting microtubules for cancer chemotherapy. *Curr Med Chem Anticancer Agents.* 2005; 5: 65–71.
28. **Stehn JR, Schevzov G, O'Neill GM, et al.** Specialisation of the tropomyosin composition of actin filaments provides new potential targets for chemotherapy. *Curr Cancer Drug Targets.* 2006; 6: 245–56.
29. **De Martino A, Filomeni G, Aquilano K, et al.** Effects of water garlic extracts on cell cycle and viability of HepG2 hepatoma cells. *J Nutr Biochem.* 2006; 17: 742–9.
30. **Xiao D, Pinto JT, Soh JW, et al.** Induction of apoptosis by the garlic-derived compound S-allylmercaptocysteine (SAMC) is associated with microtubule depolymerization and c-Jun NH-terminal kinase 1 activation. *Cancer Res.* 2003; 63: 6825–37.
31. **Xiao D, Pinto JT, Gundersen GG, et al.** Effects of a series of organosulfur compounds on mitotic arrest and induction of apoptosis in colon cancer cells. *Mol Cancer Ther.* 2005; 4: 1388–98.
32. **Hosono T, Fukao T, Ogihara J, et al.** Diallyl trisulfide suppresses the proliferation and induces apoptosis of human colon cancer cells through oxidative modification of beta-tubulin. *J Biol Chem.* 2005; 280: 41487–93.
33. **Prager-Khoutorsky M, Goncharov I, Rabinkov A, et al.** Allicin inhibits cell polarization, migration and division via its direct effect on microtubules. *Cell Motil Cytoskeleton.* 2007; 64: 321–37.
34. **Hosono T, Hosono-Fukao T, Inada K, et al.** Alkenyl group is responsible for the disruption of microtubule network formation in human colon cancer cell line HT-29 cells. *Carcinogenesis.* 2008; 29: 1400–6.
35. **Sela U, Ganor S, Hecht I, et al.** Allicin inhibits SDF-1alpha-induced T cell interactions with fibronectin and endothelial cells by down-regulating cytoskeleton rearrangement, Pyk-2 phosphorylation and VLA-4 expression. *Immunology.* 2004; 111: 391–9.
36. **Binder LI, Frankfurter A, Rebhun LI.** The distribution of tau in the mammalian central nervous system. *J Cell Biol.* 1985; 101: 1371–8.
37. **Fulga TA, Elson-Schwab I, Khurana V, et al.** Abnormal bundling and accumulation of F-actin mediates tau-induced neuronal degeneration *in vivo*. *Nat Cell Biol.* 2007; 9: 139–48.
38. **Canu N, Dus L, Barbato C, et al.** Tau cleavage and dephosphorylation in cerebellar granule neurons undergoing apoptosis. *J Neurosci.* 1998; 18: 7061–74.
39. **Rametti A, Esclaire F, Yardin C, et al.** Linking alterations in tau phosphorylation and cleavage during neuronal apoptosis. *J Biol Chem.* 2004; 279: 54518–28.
40. **Merrick SE, Demoise DC, Lee VM.** Site-specific dephosphorylation of tau protein at Ser202/Thr205 in response to microtubule depolymerization in cultured human neurons involves protein phosphatase 2A. *J Biol Chem.* 1996; 271: 5589–94.
41. **Davis DR, Brion JP, Couck AM, et al.** The phosphorylation state of the microtubule-associated protein tau as affected by glutamate, colchicine and beta-amyloid in primary rat cortical neuronal cultures. *Biochem J.* 1995; 309: 941–9.
42. **Mattson MP.** Effects of microtubule stabilization and destabilization on tau immunoreactivity in cultured hippocampal neurons. *Brain Res.* 1992; 582: 107–18.
43. **Carri MT, Ferri A, Battistoni A, et al.** Expression of a Cu,Zn superoxide dismutase typical of familial amyotrophic lateral sclerosis induces mitochondrial alteration and increase of cytosolic Ca²⁺ concentration in transfected neuroblastoma SH-SY5Y cells. *FEBS Lett.* 1997; 414: 365–8.
44. **Aquilano K, Rotilio G, Ciriolo MR.** Proteasome activation and nNOS down-regulation in neuroblastoma cells expressing a Cu,Zn superoxide dismutase mutant involved in familial ALS. *J Neurochem.* 2003; 85: 1324–35.
45. **Vigilanza P, Aquilano K, Rotilio G, et al.** Transient cytoskeletal alterations after SOD1 depletion in neuroblastoma cells. *Cell Mol Life Sci.* 2008; 65: 991–1004.
46. **Lowry OH, Rosebrough NJ, Farr AL, et al.** Protein measurement with the Folin phenol reagent. *J Biol Chem.* 1951; 193: 265–75.
47. **Gamblin TC, Chen F, Zambrano A, et al.** Caspase cleavage of tau: linking amyloid and neurofibrillary tangles in Alzheimer's disease. *Proc Natl Acad Sci USA.* 2003; 100: 10032–7.
48. **Morris EJ, Evason K, Wiand C, et al.** Misdirected vimentin messenger RNA alters cell morphology and motility. *J Cell Sci.* 2000; 113: 2433–43.
49. **Nicoletti I, Migliorati G, Pagliacci MC, et al.** A rapid and simple method for measuring thymocyte apoptosis by propidium iodide staining and flow cytometry. *J Immunol Methods.* 1991; 139: 271–9.
50. **Basu A, Haldar S.** Microtubule-damaging drugs triggered bcl2 phosphorylation-requirement of phosphorylation on both serine-70 and serine-87 residues of bcl2 protein. *Int J Oncol.* 1998; 13: 659–64.
51. **Pathan N, Aime-Sempe C, Kitada S, et al.** Microtubule-targeting drugs induce bcl-2 phosphorylation and association with Pin1. *Neoplasia.* 2001; 3: 550–9.
52. **Johnson GV.** Tau phosphorylation and proteolysis: insights and perspectives. *J Alzheimers Dis.* 2006; 9: 243–50.
53. **Tanaka T, Zhong J, Iqbal K, et al.** The regulation of phosphorylation of tau in SY5Y neuroblastoma cells: the role of protein phosphatases. *FEBS Lett.* 1998; 426: 248–54.
54. **Tian Q, Wang J.** Role of serine/threonine protein phosphatase in Alzheimer's disease. *Neurosignals.* 2002; 11: 262–9.
55. **Davis DR, Anderton BH, Brion JP, et al.** Oxidative stress induces dephosphorylation of tau in rat brain primary neuronal cultures. *J Neurochem.* 1997; 68: 1590–7.
56. **Galas MC, Dourlen P, Begard S, et al.** The peptidylprolyl cis/trans-isomerase Pin1 modulates stress-induced dephosphorylation of Tau in neurons. Implication in a pathological mechanism related to Alzheimer disease. *J Biol Chem.* 2006; 281: 19296–304.
57. **Zambrano CA, Egana JT, Nunez MT, et al.** Oxidative stress promotes tau

- dephosphorylation in neuronal cells: the roles of cdk5 and PP1. *Free Radic Biol Med.* 2004; 36: 1393–402.
58. **Sommer D, Coleman S, Swanson SA, et al.** Differential susceptibilities of serine/threonine phosphatases to oxidative and nitrosative stress. *Arch Biochem Biophys.* 2002; 404: 271–8.
59. **Aggen JB, Nairn AC, Chamberlin R.** Regulation of protein phosphatase-1. *Chem Biol.* 2000; 7: R13–23.
60. **Agarwal-Mawal A, Paudel HK.** Neuronal Cdc2-like protein kinase (Cdk5/p25) is associated with protein phosphatase 1 and phosphorylates inhibitor-2. *J Biol Chem.* 2001; 276: 23712–8.
61. **Li M, Ciu JR, Ye Y, et al.** Antitumor activity of Z-ajoene, a natural compound purified from garlic: antimitotic and microtubule-interaction properties. *Carcinogenesis.* 2002; 23: 573–9.
62. **Dalle-Donne I, Rossi R, Giustarini D, et al.** Actin carbonylation: from a simple marker of protein oxidation to relevant signs of severe functional impairment. *Free Radic Biol Med.* 2001; 31: 1075–83.
63. **Johnson GV, Jenkins SM.** Tau protein in normal and Alzheimer's disease brain. *J Alzheimers Dis.* 1999; 1: 307–28.
64. **Avila J, Lucas JJ, Perez M, et al.** Role of tau protein in both physiological and pathological conditions. *Physiol Rev.* 2004; 84: 361–84.
65. **Mills JC, Lee VM, Pittman RN.** Activation of a PP2A-like phosphatase and dephosphorylation of tau protein characterize onset of the execution phase of apoptosis. *J Cell Sci.* 1998; 111: 625–36.